Controlling weathering and erosion intensity on the southern slope of the Central Himalaya by the Indian summer monsoon during the last glacial

Kuwahara, Yoshihiro
Department of Environmental Changes, Faculty of Social and Cultural Studies, Kyushu University

Masudome, Yukiko
Department of Environmental Changes, Faculty of Social and Cultural Studies, Kyushu University

Paudel, Mukunda Raj
Department of Environmental Changes, Faculty of Social and Cultural Studies, Kyushu University

Fujii, Rie
Department of Geology and Mineralogy, Division of Earth and Planetary Sciences, Graduate School of Science | Department of Environmental Changes, Faculty of Social and Cultural Studies, Kyushu University

他

https://hdl.handle.net/2324/26645

出版情報：Global and Planetary Change. 71 (1/2), pp.73-84, 2010-03-01. Elsevier
バージョン：

Controlling weathering and erosion intensity on the southern slope of the Central Himalaya by the Indian summer monsoon during the last glacial

Yoshihiro Kuwahara[a], Yukiko Masudome[a], Mukunda Raj Paudel[a,b], Rie Fujii[a,c], Tatsuya Hayashi[a,d], Mami Mampuku[a] and Harutaka Sakai [a,c]

[a] Department of Environmental Changes, Faculty of Social and Cultural Studies, Kyushu University, Motooka, Fukuoka 819-0395, Japan.
E-mail: ykuwa@scs.kyushu-u.ac.jp

Present address:
[b] Department of Geology, Tribhuvan University, Trichandra Campus, Ghantaghar, Kathmandu, Nepal.

[c] Department of Geology and Mineralogy, Division of Earth and Planetary Sciences, Graduate School of Science, Kyoto University, Kyoto 606-8502, Japan.

[d] National Museum of Nature and Science, Department of Geology and Paleontology, Division of Paleoenvironment and Paleoecology, Hyakunin-cho 3-23-1, Shinjuku-ku, Tokyo 169-0073, Japan

Corresponding author:
Yoshihiro Kuwahara
Department of Environmental Changes, Faculty of Social and Cultural Studies, Kyushu University, Motooka, Fukuoka 819-0395, Japan.
E-mail: ykuwa@scs.kyushu-u.ac.jp
TEL:+81-92-802-5654
FAX:+81-92-802-5662

Abstract

This paper reports the results of clay mineral analysis (the amount of clay fraction, clay mineral assemblages, illite crystallinity) of samples collected from a drilled core (Rabibhawan (RB) core) located in the west-central part of the Kathmandu Basin on the southern slope of the Central Himalaya. The amount of clay fraction in the core sediments between 12 m and 45 m depth (corresponding to ca. 17 ~ 76 ka), which belong to the Kalimati Formation, is variable and shows three clay-poor zones (19 ~ 31 ka, 44 ~ 51 ka, and 66 ~ 75 ka). The variations correspond with those of illite crystallinity index (Lanson index (LI) and modified Lanson index (MLI)) and kaolinite/illite ratio as well as the fossil pollen and diatom records reported by previous workers. These data reveal the following transformations occurring during the weathering process in this area:

micas (mainly muscovite) $\rightarrow$ illite
($\rightarrow$ illite-smectite mixed layer mineral (R=1)) $\rightarrow$ kaolinite.

The sedimentation rate (~ 50 cm/kyr) of clay-poor zones that correspond to dry climate intervals is only half that of clay-rich zones (~ 120 cm/kyr) that correspond to wet climate intervals, indicating weakened chemical weathering and erosion and low suspended discharge during dry climate intervals. The clay-poor zones commonly show unique laminite beds with very fine, authigenic calcite, which was probably precipitated under calm and high calcite concentration conditions caused by low precipitation and run-off.

The variations between dry and wet conditions in this area as deduced from clay minerals appear to follow the Indian Summer Monsoon Index (ISMI) (30°N – 30°S, 1 July) and northern hemisphere summer insolation (NHSI) signals (30°N) at 1 July, especially during the dry climate zones, whereas the wet maxima of the wet climate zones somewhat deviate from the strongest NHSI. On the other hand, the dry-wet records lead markedly the SPECMAP stack (by about 5,000 years). These results suggest that the Indian summer monsoon precipitation was strongly controlled by the NHSI or summer insolation difference between the Himalayan-Tibetan Plateau and the subtropical Indian Ocean, showing a major fluctuation on the 23,000 years precessional cycle, and that it was not driven by changes in high-latitude ice volume, although the records of clay mineral indices during the wet intervals leave a question that other factors, in addition to insolation forcing, may play important roles in weathering, erosion, and sedimentation processes.

Keywords: Indian monsoon, last glacial, paleoclimate, weathering, clay minerals, Nepal Himalaya.

1. Introduction

The Indian monsoon system is one of the major weather systems on the Earth and affects most densely populated regions. Differential heating during summer results in a seasonal low pressure cell over the Indian continental landmass and a high pressure cell over the cooler Indian Ocean. As a consequence, warm humid southwest summer winds from the Indian Ocean flow onshore and contribute most to the rainfall (Colin et al., 1998; Kudrass et al., 2001; Rashid et al., 2007). Most of the monsoonal precipitation falls on the catchments of the Ganges-Brahmaputra-Meghna (GBM) river system, whose rivers drain most of the Himalayas and the northern Indian subcontinent (Kudrass et al., 2001; France-Lanord et al., 2003; Rashid et al., 2007). Water and suspended discharge of the river system, therefore, get concentrated during only five months (June to October) of the summer monsoon (Islam et al., 2002; Goodbred, 2003). Natural calamities, such as flooding or landslide, are also more frequent during this season (Rashid et al, 2007).

It is naturally expected that past modifications of the intensity of chemical and physical weathering and erosion of the Himalayan and Burman ranges and the GBM catchments are strongly related to past variations in the strength of the Indian summer monsoon (Colin et al. 1998). It is known that numerous paleoclimatic studies, based on several proxies such as % *Globigerina bulloides*, organic carbon content, lithogenic grain size, and pollen content, have permitted reconstruction of changes in the paleo-monsoon intensity (e.g., Anderson and Prell, 1993; Sirocko et al., 1993; Overpeck et al., 1996; Schulz et al., 1998; Ivanochko et al., 2005). These proxies, however, are generally of monsoon wind strength and monsoon wind-induced upwelling, rather than precipitation (Tiwari et al., 2006; Rashid et al., 2007; Shakun et al., 2007). Rashid et al. (2007) state that summer monsoonal precipitation on the Indian subcontinent is not linearly correlated to wind strength, because it depends on the moisture content of the incoming monsoon winds, which is determined by sea surface temperature (SST) in the southern hemisphere and by the convergence and rate of ascent of the air parcels after they cross the Indian coast. On changes in the strength of the Indian summer monsoon precipitation or in the intensity of weathering and erosion induced by precipitation, continental records from the Himalayas and the north Indian subcontinent, where Indian summer monsoon winds blow directly, are extremely rare (Sinha et al., 2005), while the records from marine sediments are many (e.g., Bay of Bengal and Andaman Sea: Colin et al., 1998, 1999; Rashid et al., 2007, Arabian Sea: Sirocko et al., 1991, 1993, 2000; Tiwari et al., 2006).

Precipitation plays a key role in the formation, weathering, erosion and transport of clay minerals to the depositional basins (Singer, 1984; Chamley, 1989; Robert, 2004). Therefore, clay minerals can be useful indicators of paleoclimatic conditions and have been used to estimate the intensity of precipitation or continental wetness (Robert and Kennett, 1994; Diester-Haass et al., 1998; Robert, 2004). However, paleoclimatic interpretation of clay minerals or other mineralogical indices such as grain size in sediments, especially of those transported from large source areas such as the Himalayas and the northern Indian subcontinent to the Indian Ocean, is anything but straightforward. This is because weathering, erosion, transport and sedimentation processes are controlled by many factors (e.g., mixing of exotic minerals, selective erosion and transport, mixing of detrital and authigenic clay minerals, asynchronous weathering and transport/deposition) (Singer, 1984; Chamley, 1989).

Moreover, Kübler Index (KI) (Kübler, 1964), which is conventional illite crystallinity index defined by the full width at half maximum intensity (FWHM) of 10 Å illite X-ray diffraction (XRD) peak and has extensively been used to reconstruct the paleoclimate (*e.g.*, Chamley 1989; Fukuzawa et al. 1997; Lamy et al. 2000), is not always available for estimation of illite crystallinity (Srodon, 1979, Srodon and Eberl, 1984; Lanson, 1997; Kuwahara et al., 2001). According to

Srodon (1979), the KI is significantly larger for finer fractions because the FWHM of the illite 001 peak is mostly a function of the amount and composition of the illite-smectite mixed layer (I-S) component of the sample and the I-S component has a finer particle size than illite. To overcome this problem, Lanson (1997) proposed a new illite crystallinity index (Lanson index (LI)), which accounts for the relative proportion of illite crystallites with low coherent scattering domain size (CSDS), by using decomposition procedure of X-ray diffraction (XRD) patterns. The asymmetry of the complex 001 XRD peaks of illitic minerals near 10 Å is in fact due to the presence of different mineral phases with different illite content and different CSDS thickness (Lanson, 1997). Therefore, he decomposed the complex peaks using three elementary peaks corresponding to three different phases with different illite content and different CSDS thickness, that is, I-S, poorly crystallized illite (PCI), and well-crystallized illite (WCI). The LI can be determined by the characteristics of the three elementary peaks. The modified Lanson index (MLI), which estimates illite crystallinity only from the difference between PCI and WCI, is available for the estimation of variations in weathering and hydrolysis conditions (Kuwahara et al., 2001).

The Kathmandu Basin is one of the ideal targets for studying the variations in the Indian monsoon climate and their bearing on the uplifting of the Himalayan-Tibetan orogen, because the basin is located on the southern slope of the central Himalaya and filled with a thick pile of Late Pliocene to Quaternary sediments (Sakai et al., 2001a, b; Fujii and Sakai, 2001). The Kathmandu Basin is also ideal for interpretation of paleoclimates from clay minerals in sediments, because the basin has a diameter of only about 30 km and the river's catchment area is confined to the inside slope of the basin, implying that the basin-fill sediments are supplied only from the mountains surrounding the basin (Sakai, 2001; Kuwahara et al., 2001). Yet, previous studies could not completely decipher the paleoclimatic changes in the Kathmandu Basin, because of discontinuities in the surface exposures sampled (Yoshida and Igarashi, 1984; Igarashi et al., 1988; Nakagawa et al., 1996; Goddu et al., 2007). The scientific group of this study conceived the "Paleo-Kathmandu Lake (PKL) project", under which they carried out academic drilling in the Kathmandu Basin, Nepal Himalaya, and investigated the cores and surface exposures from various viewpoints and by different methods (Sakai, 2001). Several earlier workers reported on the results of fossil pollen, fossil diatom and organic geochemical analyses and sediment characteristics from surface geological surveys of the Kathmandu basin and studies of the drill cores obtained from the basin (Sakai et al., 2001a, b, Fujii and Sakai, 2001, 2002, Maki et al., 2002, Fujii et al., 2004, Hayashi et al., 2007a, b, Mampuku et al., 2008 ; Hayashi et al., 2009). In this paper, it is attempted to reconstruct the variations in the intensity of weathering and erosion conditions, as recorded in the clay minerals of the sediments from the Kathmandu Basin. The variations were probably controlled by Indian summer monsoon precipitation during the past 76,000 years.

2. Materials and methods

2.1. Sample preparation and XRD measurements

The materials used were a 218 m long core (RB core), which was obtained from drilling at Rabibhawan in the west-central part of the Kathmandu Basin under the PKL Project in 2000 (Sakai et al., 2001b) (Fig. 1). For clay mineral analysis, core sediment samples, collected at 10 cm interval between 7 m and 45 m depth, were used. The topmost part of the sampled core, from 7 m to 11 m depth, is composed of medium-to very coarse-grained micaceous granitic sand beds of the Patan Formation, which corresponds to the sediments of the Bagmati river (Sakai et al., 2001b) (Fig. 2). The sediments immediately below this zone belong to the Kalimati Formation, and those between 12 m and 45 m depth are of organic black or dark gray mud, known as "Kalimati Clay". The top 1 m part of the Kalimati Formation, which probably corresponds to the period covering the draining out of lake water, is characterized by thin interbeds of silt and sand (for further details of the RB core, see Sakai et al., 2001b). The chronology of the RB core has been constructed by Hayashi et al. (2009), Mampuku et al. (2008) and Hayashi (2007) using ^{14}C accelerator mass spectroscopy (AMS) dating and fine tuning of a pollen wet and dry index record to the SPECMAP $\delta^{18}O$ stack record (Imbrie et al., 1984). Their age-depth model of the RB core gives 15 ka at 11 m depth, which marks the boundary between the Patan and the Kalimati Formations, and 76 ka at 45 m depth (Fig. 3).

Each sample was first dried in an air-bath at 60°C for one day and then weighed. The clay fraction under 2μm was separated from each sample by gravity sedimentation. Then, about 200 mg of this fraction was collected by the Millipore® filter transfer method using the Gelman® GA-9, 0.45 μm pore, 47 mm diameter Metricel© filter to provide optimal orientation (Moore and Reynolds, 1989). The thickness of the clay cake formed on the filter was over 15 mg/cm^2, which was adequate for XRD quantitative analysis (Moore and Reynolds, 1989). The clay cake was then transferred onto a glass slide. For each sample, both air-dried (AD) and ethylene glycol solvated (EG) preparations were made. The EG preparation was carried out to expose the sample to the vapor of the reagent in desiccator for over 8 hrs at 60°C. On the other hand, the non-clay fraction of over 2μm size was dried and weighed to estimate the amount of the clay fraction.

All the XRD data were collected on a Rigaku X-ray Diffractometer RINT 2100V, using CuKα radiation monochromatized by a curved graphite crystal in a step of 0.02° with a step-counting time of 4 seconds.

2.2. XRD Decomposition and clay mineral analysis

The decomposition (profile fitting) procedure of Lanson (1997) was followed to obtain peak position, FWHM, and intensity (peak area) for each elementary peak, which were used for determination of the percentages of clay minerals and illite crystallinity. The XRD raw data were converted into ASCII format, transferred to an Apple Power Macintosh computer, and treated with a scientific graphical analysis program XRD MacDiff (Petschick, 2000). Basically, the treatment of a raw file begins with preliminary smoothing to decrease the effect of statistical counting errors. Then, a background was subtracted to eliminate most of its contribution to the peaks. Finally, the elementary peak fitting was done. All decompositions were performed with symmetrical elementary peaks with Gaussian shape. Fig. 4 shows a result of decomposition with five elementary peaks which correspond to smectite, chlorite, I-S (R=1), PCI and WCI, for the XRD pattern of AD sample. To check the reproducibility and detect the errors in the procedure, the decomposition was repeated four times for an XRD pattern of each sample and was also performed for four XRD patterns collected for each given sample. The errors on the measurement of FWHM and peak area were < 1% and <3%, respectively.

The percentage of each clay mineral in the core sediment samples was determined by the Mineral Intensity Factor (MIF) method (Moore and Reynolds, 1989):

$$CM_i\ (\%) = 100 \times (I_i / MIF_i) / \sum (I_i / MIF_i) \quad (i = 1, 2, \cdots n) \qquad (1)$$

where CM_i is the percentage of clay mineral *i* and I_i is an integrated peak intensity for clay mineral *i*. The quantity MIF_i is the calibration constant for the diffraction peak used for clay mineral *i* that allows for quantitative estimation of its proportion in a mixture with clay mineral *i'*, and can be written as:

$$MIF_i = MRI_i / MRI_{i'} \qquad (2)$$

where MRI_i, called Mineral Reference Intensity, is the theoretical integrated intensity of clay mineral *i* under specified instrumental operating conditions. MRI was calculated by the computer program NEWMOD© (Reynolds and Reynolds, 1996), following the procedure suggested by Moore and Reynolds (1989). Note that the procedure forces the analysis to total 100%.

Illite crystallinity was estimated using the LI (Lanson, 1997) and MLI (Kuwahara et al., 2001). The LI is expressed thus:

$$LI = 0.1/[\text{PCI peak relative intensity} \times \text{PCI peak FWHM} \times (\text{PCI peak position} - \text{WCI peak position})] \quad (3)$$

where

$$\text{PCI peak relative intensity} = \text{PCI intensity} / (\text{PCI intensity} + \text{WCI intensity} + \text{I-S intensity}). \quad (4)$$

The MLI is defined thus:

$$MLI = \text{PCI peak relative intensity} \times \text{PCI peak FWHM} \times (\text{PCI peak position} - \text{WCI peak position})] \quad (5)$$

where

$$\text{PCI peak relative intensity} = \text{PCI intensity} / (\text{PCI intensity} + \text{WCI intensity}). \quad (6)$$

It is to be noted that the higher LI and the lower MLI, indicate higher illite crystallinity.

3. Results

The amount of the clay fraction in the core sediments of the Kalimati Formation between 12 m and 45 m depth varies between 2 wt% and 34 wt%, with an average of 14 wt%. In the topmost part between 7 m and 12 m depth, which is composed of the sandy beds of the Patan Formation and the topmost part of the Kalimati Formation, the amount of clay fraction is much less (1 ~ 8 wt%, average 5 wt%) (Fig.5a). The Kalimati Formation between 12 m and 45 m depth consists of three clay-poor zones (17.8 ~ 22.0 m, 30.8 ~ 33.2 m and 41.1 ~ 44.8 m in depth) in which the amount of clay minerals is almost less than the average, except in some thin clay-enriched parts. The poorest part of the clay fraction in the clay-poor zones is at 19.6 ~ 22.0 m depth. In the other zones, the clay fraction varies around the average (14 wt%) at relatively short intervals (0.4 ~ 1 m), with some clay-rich peaks (> 20 wt%).

The clay minerals in the core sediments include illite, kaolinite, chlorite, I-S (R=1), and smectite (Figs. 5c and 6). Among these, illite is the most dominant one (50 ~ 80% in the clay fraction, average 61%), followed by kaolinite (7 ~ 30% in the clay fraction, average 19%). The morphology and crystal structure (polytype) of illite in the basin sediments clearly suggest that the illite is detrital (Kuwahara, 2006). The curve depicting the variations in the percentage of illite is a mirror image of the corresponding curve for kaolinite. Chlorite (3 ~ 9% in the clay fraction), I-S (R=1) (4 ~ 12% in the clay fraction), and smectite (traces to 8% in the clay fraction) are of lesser importance in the clay fraction. In addition, the amounts of the three clay minerals “in the sediments” are extremely low; it is particularly so of smectite whose amount does not reach even 1 wt% (Fig. 5d). Besides the clay minerals, the sediments are composed of detrital and precipitated minerals (quartz, feldspars, micas, calcite) (Paudel et al., 2004), amorphous silica (diatom shell) (Hayashi, 2007; Hayashi et al., 2009), and organic materials (Mampuku et al., 2008).

The illite crystallinity indices (LI and MLI) also appear to vary in accordance with the variations in the amount of the clay fraction or of illite and kaolinite (Fig. 5b). The MLI in the Kalimati Formation varies between 0.1 and 0.27, with an average of 0.17. In the high illite crystallinity zones (17.8 ~ 21.7 m, 30.6 ~ 33.0 m and 39.8 ~ 44.5 m depth), the MLI is almost less than the average, except in certain zones where some peaks can be seen denoting slightly high MLI. These three high illite crystallinity zones overlap the three clay-poor zones mentioned above. The MLI in the other zones appears to fluctuate around the average at relatively short intervals (0.4 ~ 1 m), with some high peaks (> 0.2) that indicate low illite crystallinity.

4. Discussion

4.1. Weathering and erosion processes in the Kathmandu Basin

The detrital minerals in the Kathmandu Basin sediments are mostly micas (mainly muscovite), feldspars and quartz for which the source rocks could have been the gneisses and granites of the Shivapuri injection complex and weakly metamorphosed rocks of the Phulchauki Group (Sakai, 2001). Besides these, no other source rock, such as hydrothermal ore body, which could have contributed clay minerals, is known from or near the basin. The illitic minerals – the most dominant clay minerals – in the basin sediments, therefore, could have been formed by the exfoliation of micas during weathering, and were eroded and transported from the surrounding mountains by rainfall and run-off. In the Kalimati Formation, the percentage of illite in the clay fraction decreases with increase in the total amount of the clay fraction (Figs. 5a and c, Fig. 7(e)). In addition, illite crystallinity becomes low when the percentage of illite in the clay fraction decreases (Fig. 7(d); note that the higher MLI indicate lower illite crystallinity). Hence, while the amount of clay minerals fed to the Kathmandu Basin, increased with intensification of chemical weathering or hydrolysis, the amount and crystallinity of illite, derived from parent micas, are expected to have been reduced.

Kaolinite, the other dominant clay mineral in the basin sediments, and I-S (R=1) have clear negative correlations with illite (Figs. 7(a) and (b)). That is, the amount of kaolinite, as also of I-S (R=1), increases with decrease in the amount of illite, while the amount of clay minerals increases in and around the Kathmandu Basin (Figs. 5 and 7). Kaolinite is typical of warm and humid areas with good drainage conditions (Robert, 2004). Precipitation plays a key role in mineral deposition by exposing fresh rock and mineral surfaces to chemical and physical weathering and transporting the eroded minerals to the depositional basins. Steep continental relief reinforces the role of precipitation and run-off in chemical weathering and erosion (Chamley, 1989; Robert, 2004). Therefore, warm and wet conditions and steep relief in and around the Kathmandu Basin could have contributed to the formation of kaolinite.

Smectite in the clay fraction has no correlation with illite (Fig. 7(c)). In addition, the amount of smectite in the Kalimati Formation does not anywhere reach even 1 wt% (Fig. 5(d)). Smectite, therefore, can not be considered the main clay mineral or the main secondary clay mineral to have been derived from alteration of illite in the Kathmandu Basin, although it is also indicative of warm and intense chemical weathering. This does not, however, contradict that smectite occurs in areas of low, rather than steep, relief characterized by alternating episodes of precipitation and aridity (Chamley, 1989, Robert, 2004).

Based on these facts, the following transformations are inferred to have taken place in this area during the weathering process:

micas (mainly muscovite) $\rightarrow$ illite
($\rightarrow$ illite-smectite mixed layer mineral (R=1)) $\rightarrow$ kaolinite.

Also, during this process, the feldspars must have altered mainly to kaolinite (Chamley, 1989). With intensification of chemical weathering and consequent erosion in and around the Kathmandu Basin, hydrolysis and leaching of parent minerals were activated, followed by degradation of illite – derived from alteration of micas – (lowering of crystallinity and transformation to I-S), and finally the formation of kaolinite via illitic minerals (illite and I-S). With the waning of chemical weathering and erosion, the formation of clay minerals and the transformation of parent minerals to kaolinite would slow down, and consequently the clay mineral content in the sediments would decrease, resulting in a low kaolinite to illite ratio.

Also, the sedimentation rates differ between intensified and weakened chemical weathering and erosion conditions. Based on the age-depth model of the RB core (Hayashi et al., 2009; Mampuku et al., 2008; Hayashi, 2007), the average sedimentation rate in the clay-poor zone, between 18 m and 22 m depth (ca. 19 ~ 31 ka), is estimated to be about 50 cm/kyr, and that in the clay-rich parts (13 ~ 18 m (17 ~ 19 ka) and 22 ~ 28 m (31 ~ 44 ka)), below and above the clay-poor zone, are about 100 cm/kyr, twice that in the clay-poor zone (Fig. 8). Unfortunately, the details of the sedimentation rates between 28 m and 45 m depth (44 ~ 76ka) are unclear because the age between them is based only on one single datum (tie-point between 47.5 m depth and MIS 5.1 (81 ka) (Hayashi et al., 2009)). However, it is certain that the sedimentation rate in the clay-rich zone was faster than that in the clay-poor zone. Supposing that the sedimentation rate in the clay-rich zone below 28 m depth was twice as much as that in the clay-poor zone, in the same way as above 28 m depth, the former is estimated to be about 60 cm/kyr and the latter is about 30 cm/kyr (Fig. 8).

In the clay-poor zones corresponding to weakened chemical weathering and erosion conditions (or dry climate), unique laminite beds with alternating very thin white calcite-rich and black carbonaceous clayey layers (20 ~ 30 pairs/cm), which are not contradictory to the low sedimentation rates in the clay-poor zones, are recognized (Sakai, 2001; Paudel et al., 2004; Kuwahara, 2006). Paudel et al. (2004) and Kuwahara (2006) have reported that the calcite particles in the laminite beds are very fine (~ 50 µm), euhedral, and authigenic (precipitated in lake water). The calcite could have been formed under conditions tranquil enough to facilitate formation of laminite beds, when calcite concentration in lake water was high because of low precipitation and run-off and consequent shrinkage of the Paleo-Kathmandu Lake during dry climates. The fossil diatom study on the same core yielded similar evidence of falling lake-level during the dry climate intervals (Hayashi, 2007; Hayashi et al., 2009). Also, calcite formation was reported by the mineralogical study of the JW-3 core, which was drilled near the RB core site (Fujii et al., 2001). Such authigenic calcite in the Kathmandu Basin sediments, therefore, serves not only as an important indicator of dry climate but also as a key mineral in correlation of (core) sediments.

4.2. Variations in dry-wet conditions in the Kathmandu Basin and monsoonal response to insolation forcing

From the results of clay mineral analysis of the Kathmandu Basin sediments, three main dry climate intervals (clay-poor, high illite crystallinity, low kaolinite/illite (K/I) ratio zones) and four wet climate intervals (clay-rich, low illite crystallinity, high K/I ratio zones) were recognized between 17 and 76 ka. The three dry climate intervals are estimated to be 19 ~ 31 ka, 44 ~ 51 ka, and 66 ~ 75 ka (Fig. 8). The records prior to 17 ka (in the topmost part between 7 m and 12 m depth, which is composed of the sandy beds of the Patan Formation and the topmost part of the Kalimati Formation) are not suitable for the reconstruction of paleoclimate. The variation record of dry-wet climate in and around the Kathmandu Basin depicted by the clay mineral proxies (e.g., the K/I ratio) is very similar to that revealed by the pollen analysis of the same core (Fujii et al., 2004) (Fig. 8).

In the variation record of dry-wet climate in this area, one can observe a strong long-term variation in the 23,000 years precessional cycle of solar radiation, as dry maxima are centered around 25, 47 and 70 ka, corresponding to the northern hemisphere summer insolation (NHSI) signal (Fig. 8). Similar results have been obtained by the $\delta^{18}O$ record of the planktonic foraminifera *Globigerinoides ruber* (Schultz et al, 1998) and carbonate content (Leuschner and Sirocko, 2003) in the sediment cores of the Arabian Sea. The maximum signal at 47 ka is not seen in the SPECMAP stack or GISP2 $\delta^{18}O$ records (Blunier and Brook, 2001). These signals around Marine Isotope Stage (MIS) 3 may be of regional significance to Indian monsoonal variability (Schulz et al., 1998). The dry maximum signal around 25 ka is consistent with the coldest part, which corresponds to the last glacial maximum (LGM), as revealed by the pollen analysis of the same core (Fujii et al., 2004).

Leuschner and Sirocko (2003) constructed an Indian Summer Monsoon Index (ISMI) that is defined as the insolation difference between 30°N and 30°S on 1 August, based on the fact that the modern Indian summer monsoon is mainly driven by low pressure over the Himalayan-Tibetan Plateau and high pressure over the southern subtropical Indian Ocean. The ISMI or NHSI signal (21 June, perihelion) showing the 23,000 years precessional tempo, leads the global ice volume record as indicated by the SPECMAP stack by several thousand years (Ruddiman, 2001, Leuschner and Sirocko, 2003, Wang et al., 2005). Further, Clemens and Prell (2003) show that Arabian Sea summer monsoon stack and factor lag behind the NHSI signal (21 June, perihelion) by about 8,000 years and behind the ice volume record by about 3,000 years, at the precession band (23 kyr). Similar results on the long lag of the monsoon record were also obtained from the windblown lake diatoms in the sediment cores from the tropical Atlantic Ocean, as a proxy of the North African monsoon (lagging behind the NHSI (21 June, perihelion) by 5,000 ~ 6,000 years) (Pokras and Mix, 1987). Ruddiman (1997, 2001), however, suggests that the net lag of the North African monsoon signal behind the NHSI (21 June, perihelion) is probably only 1,000 ~ 2,000 years (not 5,000 ~ 6,000 years) because of the delayed diatom deposition in the Atlantic Ocean.

The variation records of dry-wet condition in this area, deduced from clay minerals as well as fossil pollen proxies, appear to follow the summer insolation with no long lag, especially from the coincidence of the dry climate zones and the low ISMI and NHSI intervals (Fig. 8) and the results of the cross-correlation analysis of the NHSI with the record of the K/I ratio (Fig. 9). The ISMI and NHSI in Fig. 8 were recalculated using the 1 July summer insolation signal, because nowadays the summer monsoon precipitation in this area reaches its peak in July (Meteorological Forecasting Division, Government of Nepal, 2006). We also show in Fig. 8 variation curves of the K/I ratio and pollen dry index depicted based on the age model reconstructed using the sedimentation rates below 28 m depth of the RB core mentioned above and a tie point between 47.5 m depth and 82.5 ka corresponding to one of the maxima of the NHSI at 1 July (instead of 81 ka (MIS 5.1)), as well as those depicted using the age-depth model of Hayashi et al. (2009), Mampuku et al. (2008) and Hayashi (2007). Using the summer insolation signal at 21 June, perihelion, the dry-wet record in this area appears to lag slightly behind the NHSI (by ~ 1,000 years) (Fig 9(b)).

However, the centers (or wet maxima) of the wet climate zones depicted by the K/I ratio do not always coincide with the NHSI maxima. The wet interval between 32 and 44 ka leads the NHSI while the wet interval between 51 and 66 ka appears to lag slightly behind the NHSI (Fig. 8). These results likely show that the K/I record, especially during the wet intervals, is not as simple as a direct response to insolation forcing. Other factors, in addition to insolation forcing, may play important roles in weathering, erosion, and sedimentation processes or may complicate paleoclimatic interpretation of clay mineral (e.g., lake level change and lake water flow that affect the distribution of particle size of minerals or dispersion of clay minerals).

On the other hand, the dry-wet record leads markedly the SPECMAP stack (the ice volume record) and $\delta^{18}O$ record of the planktonic foraminifer *G. ruber* in sediment core of the Arabian Sea (Schultz et al, 1998) (by about 5,000 years) (Figs. 8 and 9(b)). Wang et al. (2005) suggest that if changes in monsoon strength take place before changes in ice volume, then monsoon variance is definitely not driven by changes in high-latitude ice volume. The results of the present study reveal that the Indian summer monsoon precipitation was strongly controlled by the northern hemisphere summer insolation or summer insolation difference between the Himalayan-Tibetan Plateau and subtropical Indian Ocean.

The question that arises here is "Why the long lag of monsoon behind the summer insolation does not show up in the clay mineral proxies of this study"? One possibility is that the samples are not from deep-sea sediments, but from intermontane basin sediments on the southern slope of the central Himalaya. For instance, the $\delta^{18}O$ of planktonic foraminifera in the sediment cores from the Indian Ocean, which was interpreted as a monsoon proxy, was certainly affected by changes in global ice volume as well as the local temperature of the Ocean water (Ruddiman, 2001). Sediment grain size or planktonic foraminifera shell flux in the deep-sea sediments was probably influenced by oceanic conditions (e.g., surface and deep-sea currents, sea-level, water temperature and chemistry) (Singer, 1984; Chamley, 1989; Tiwari et al., 2006). Such problems or intervention is not inherent in the monsoon proxies (clay minerals, fossil pollen and diatom, etc.) of the Kathmandu Basin sediments. In addition, the detritals would have transported and deposited into the Paleo-Kathmandu Lake "in an instant" as compared with those of the deep-sea sediments, because the basin had a diameter of only about 30 km and the catchment area of the river is confined to the inside slope of the basin (Sakai, 2001; Kuwahara et al., 2001). The paleo-lake sediments of the Kathmandu Basin must allow one to obtain direct and valuable information on the Indian monsoon variability.

5. Conclusions

The clay mineral study of the Paleo-Kathmandu Lake sediments reveals how the weathering processes operated in this area, how the variations in the intensity of weathering and erosion were controlled by the Indian summer monsoon precipitation, and how the Indian summer monsoon responded to the summer insolation. During the wet climate intervals, intense chemical weathering and erosion promoted the formation of clay minerals, lowered illite crystallinity, and transformed illite to kaolinite. On the other hand, during the dry climate intervals, the weakening of chemical weathering and erosion processes retarded the formation of clay minerals and the transformation of illite to kaolinite. The sedimentation rates during the wet climate intervals were roughly twice as much as those during the dry climate intervals. The variation records of dry-wet condition in this area probably follow the summer insolation with no long lag, especially during the dry climate zones, whereas the wet maxima of the wet climate zones somewhat deviate from the strongest insolation forcing. In contrast, the wet-dry records were far ahead of the SPECMAP stack (the ice volume record), indicating that the Indian summer monsoon precipitation was not driven by changes in ice volume but by the northern hemisphere summer insolation or summer insolation difference between the Himalayan-Tibetan Plateau and the subtropical Indian Ocean. It is stressed here that the comparative studies between continental and marine records will have to be pursued further for a more comprehensive understanding of the Indian summer monsoon.

7. Acknowledgements

The authors are grateful to the staff of Nissaku Co (Nepal) Pvt. Ltd. and Prof. Bishal Nath Upreti of Tribhuvan University for their many kind help. We also thank anonymous reviewers and the Editor Thomas M. Cronin for their thorough reviews that improved the quality of the study. This study was supported in part by the Grant-in-Aid for Scientific Research (Y. Kuwahara, No.17540457 and H. Sakai, No.11304030 and No.14340152) from the Japan Society for the Promotion of Science.

8. References

Anderson, D.M., Prell, W.L., 1993. A 300 kyr record of upwelling off Oman during the late Quaternary: evidence of the Asian southwest monsoon. Paleoceanography 8, 193-208.

Blunier, T., Brook, E.J., 2001. Timing of millennial-scale climate change in Antarctica and Greenland during the last glacial period. Science 291, 109-112.

Chamley, H., 1989. Clay Sedimentology. Springer-Verlag, Berlin Heidelberg.

Chelton, D.B., 1982. Statistical reliability and the seasonal cycle: comments on "Bottom pressure measurements across the Antarctic Circumpolar Current and their relation to the wind". Deep-Sea Research 29, 1381-1388.

Clemens, S.C., Prell, W.L., 2003. A 350,000 year summer-monsoon multi-proxy stack from the Owen Ridge, Northern Arabian Sea. Marine Geology 201, 35-51.

Colin, C., Kissel, C., Blamart, D., and Turpin, L., 1998. Magnetic properties of sediments in the Bay of Bengal and the Andaman Sea: impact of rapid North Atlantic Ocean climatic events on the strength of the Indian monsoon. Earth and Planetary Science Letters 160, 623-635.

Colin, C., Turpin, L., Bertaux, J., Desprairies, A., Kissel, C., 1999. Erosional history of the Himalayan and Burman ranges during the last two glacial-interglacial cycles. Earth and Planetary Science Letters 171, 647-660.

Diester-Haass, L.D., Robert, C., Chamley, H., 1998. Paleoproductivity and climate variations during sapropel deposition in the Eastern Mediterranean Sea (ODP

Leg 160). In: Emeis, K.C., Robertson, A.H.F. (Eds.), Proceedings of the Ocean Drilling Program, Scientific Results, Vol. 160. Ocean Drilling Program, College Station, TX, pp. 227-248.

France-Lanord, C., Evans, M., Hurtrez, J.E., and Riotte, J., 2003. Annual dissolved fluxes from Central Nepal rivers: budget of chemical erosion in the Himalayas. Comptes Rendus Geoscience 335, 1131-1140.

Fujii, R., Kuwahara, Y., Sakai, H., 2001. Mineral composition changes recorded in the sediments from a 284-m-long drill-well in central part of the Kathmandu Basin, Nepal. Journal of Nepal Geological Society 25, 63-69.

Fujii, R., Sakai, H., 2001. Palynological study of the drilled sediments from the Kathmandu Basin and its palaeoclimatic and sedimentological significance. Journal of Nepal Geological Society 25, 53-61.

Fujii, R., Sakai, H., 2002. Paleoclimatic changes during the last 2.5 myr recorded in the Kathmandu Basin, Central Nepal Himalayas. Journal of Asian Earth Sciences 20, 255-266.

Fujii, R., Sakai, H., Miyoshi, N., 2004. Fluctuation of Indian monsoon during the last glacial period revealed by pollen analysis of Kathmandu Basin sediments, Nepal Himalaya. Himalayan Journal of Sciences 2, 133-134.

Fukuzawa, H., Oi, K., Yamada, K., Iwata, S., Torii, M., 1997. Last 2.5 Ma changes of atmospheric circulation along the Japan Sea-Chinese Loess Plateau – the Mediterranean Sea Transect caused by uplift of the Himalayan-Tibetan Plateau. Journal of Geography 106, 204-248 (in Japanese, with English abstr.).

Goddu, S.R., Appel, E., Gautam, P., Oches, E.A., Wehland, F., 2007. The lacustrine section at Lukundol, Kathmandu Basin, Nepal: Dating and magnetic fabric aspects. Journal of Asian Earth Sciences 30, 73-81.

Goodbred, S.L.Jr., 2003. Response of the Ganges dispersal system to climate change: a source-to-sink view since the last interstade. Sedimentary Geology 162, 83-104.

Hayashi, T., 2007. Middle to Late Pleistocene monsoonal environmental changes reconstructed by fossil diatom analyses of the Paleo-Kathmandu Lake sediments, Nepal Himalaya. Ph. D. Thesis, Kyushu University. Fukuoka, Japan.

Hayashi, T., Tanimura, Y., Sakai, H., 2007a. Puncticulata versiformis sp Nov and cyclotella kathmaduensis sp Nov (Bacillariophyta), new fossil species from Pleistocene lacustrine sediments, Kathmandu, Nepal Himalaya. Journal of Phycology 43, 304-318.

Hayashi, T., Tanimura, Y., Sakai, H., 2007b. A fossil freshwater Thalassiosira, T-inlandica sp nov (Bacillariophyta), with semicontinuous cribra and elongated marginal fultoportulae. Phycologia 46, 353-362.

Hayashi, T., Tanimura, Y., Kuwahara, Y., Ohno, M., Mampuku, M., Fujii, R., Sakai, H., Yamanaka, T., Maki, T., Uchida, M., Yahagi, W., Sakai, H., 2009. Ecological variations in diatom assemblages in the Paleo-Kathmandu Lake linked with global and Indian monsoon climate changes for the last 600,000 yr. Quaternary Research (in press).

Igarashi, Y., Yoshida, M., Taabata, H., 1988. History of vegetation and climate in the Kathmandu Valley. Proceeding of Indian National Science Academy 54, A4, pp. 550-563.

Imbrie, J., Hays, J.D., Martinson, D.G., McIntyre, A., Mix, A.C., Morley, J.J., Pisias, N.G., Prell, W.L., Shackleton, N.J., 1984. The orbital theory of Pleistocene climate: Support from a revised chronology of the marine $\delta^{18}O$ record. In: Berger, N.J. (Ed), Milankovitch and Climate, Part I. Reidel, Dordrecht, pp. 269-305.

Islam, M.R., Begum, S.F., Yamaguchi, Y., and Ogawa, K., 2002. Distribution of suspended sediment in the coastal sea off the Ganges-Brahmaputra River mouth: observation from TM data. Journal of Marine Systems 32, 307-321.

Ivanochko, T.S., Ganeshram, R.S., Brummer, G.-J.A., Ganssen, G., Jung, S.J.A., Moreton, S.G., Kroon, D., 2005. Variations in tropical convection as an amplifier of global climate change at the millennial scale. Earth and Planetary Science Letter 235, 302-314.

Kübler, B., 1964. Les argiles, Indicateurs de metamorphisme. Revue De L'institut Français Du Pétrole 19, 1093-1112 (in French, with English abstr.).

Kudrass, H.R., Hofmann, A., Doose, H., Emeis, K., and Erlenkeuser, H., 2001. Modulation and amplification of climatic changes in the Northern Hemisphere by the Indian summer monsoon during the past 80 k.y. Geology 29, 63-66.

Kuwahara, Y., 2006. Reconstruction of paleoclimate recorded in clay minerals. Nendo Kagaku (Clay Science) 45, 211-219 (in Japanese).

Kuwahara, Y., Fujii, R., Sakai, H., Masudome, Y., 2001. Measurement of crystallinity and relative amount of clay minerals in the Kathmandu Basin sediments by decomposition of XRD patterns (profile fitting). Journal of Nepal Geological Society 25, 71-80.

Lamy, F., Klump, J., Hebbeln, D., Wefer, G., 2000. Late quaternary rapid climate change in northern Chile. Terra Nova 12, 8-13.

Lanson, B., 1997. Decomposition of experimental X-ray diffraction patterns (profile fitting): A convenient way to study clay minerals. Clays and Clay Minerals 45, 132-146.

Lanson, B., Besson, G., 1992. Characterization of the end of smectite-to-illite transformation: decomposition of X-ray patterns. Clays and Clay Minerals 40, 40-52.

Leuschner, D.C., Sirocko, F., 2003. Orbital insolation forcing of the Indian Monsoon – a motor for global climate changes? Palaeogeography, Palaeoclimatology, Palaeoecology 197, 83-95.

Lisiecki, L.E., Raymo, M.E., 2005. A Pliocene-Pleistocene stack of 57 globally distributed benthic $\delta^{18}O$ records. Paleoceanography 20, PA1003, doi: 10.1029/2004PA001071.

Maki, T., Fujii, R., Umeda, H., Sakai, H., Hase, Y., Shichi, K., 2004. Paleovegetation and paleoclimate in the Kathmandu Valley and Lake Baikal during the Late Quaternary. Himalayan Journal of Sciences, 2, 202.

Mampuku, M., Yamanaka, T., Uchida, M., Fujii, R., Maki, T., Sakai, H., 2008. Changes in C-3/C-4 vegetation in the continental interior of the Central Himalayas associated with monsoonal paleoclimatic changes during the last 600 kyr. Climate of the Past 4, 1-9.

Meteorological Forecasting Division, Government of Nepal, 2006. Normal (average) maximum, minimum temperature (°C) and Rainfall (mm) through 2000. http://www.mfd.gov.np/index.php.

Moore, D.M., Reynolds, R.C.Jr., 1989. X-ray Diffraction and the Identification and Analysis of Clay Minerals. Oxford University Press, New York.

Nakagawa, T., Yasuda, Y., Tabata, H., 1996. Pollen morphology of Himalayan *Pinus* and *Quercus* and its importance in palynological studies in Himalayan area. Review of Palaeobotany and Palynology 91, 317-329.

Overpeck, J., Anderson, D., Trumbone, S., Prell, W.L., 1996. The southwest Indian Monsoon over the last 18,000 years. Climate Dynamics 12, 213-225.

Paudel, M.R., Kuwahara, Y., Sakai, H., 2004. Changes in mineral composition and depositional environments recorded in the present and past basin-fill sediments of the Kathmandu Valley, central Nepal. Himalayan Journal of Science 2, 222-223.

Paillard, D., Labeyrie, L., Yiou, P., 1996. Macintosh program performs time-series analysis. EOS 77, 379.

Petschick, R., 2000. MacDiff Ver. 4.2.3, Manual. Geologisch-Paläontrologisches Institut Johann Wolfgang-Universität Frankfurt am Main Senckenberganlage 32-34, 60054 Frankfurt am Main, Germany.

Pokras, E.M., Mix, A.C., 1987. Earth’s precession cycle and quaternary climatic change in tropical Africa. Nautre 326, 486-487.

Rashid, H., Flower, B.P., Poore, R.Z., and Quinn, T.M., 2007. A 25 ka Indian Ocean monsoon variability recorded from the Andaman Sea. Quaternary Science Reviews 26, 2586-2597.

Reynolds, R.C.Jr., Reynolds, R.C.III, 1996. NEWMOD-FOR-WINDOWS™. The calculation of One-dimensional X-ray diffraction patterns of mixed-layered minerals. Reynolds, R.C.Jr., Reynolds, R.C.III, 8 Brook Road, Hanover NEW Hampshire 03755, pp. 1-25.

Robert, C., 2004. Late Quaternary variability of precipitation in Southern California and climatic implications: clay mineral evidence from the Santa Barbara Basin, ODP Site 893. Quaternary Science Reviews 23, 1029-1040.

Robert, C., Kennett, J.P., 1994. Antarctic subtropical humid episode at the Paleocene-Eocene boundary: clay mineral evidence. Geology 22, 211-214.

Ruddiman, W.F., 1997. Tropical Atlantic terrigenous fluxes since 25,000 years B.P. Marine Geology 136, 189-207.

Ruddiman, W.F., 2001. Earth's Climate, Past and Future. W.H. Freeman and Company, New York.

Sakai, H., 2001. The Kathmandu Basin: an archive of Himalayan uplift and past monsoon climate. Journal of Nepal Geological Society 25, 1-8.

Sakai, H., Fujii, R., Kuwahara, Y., 2001a. Changes of depositional system of the Palaeo-Kathmandu Lake caused by uplifting of the Nepal Lesser Himalayas. Journal of Asian Earth Sciences 20, 267-276.

Sakai, H., Fujii, R., Kuwahara, Y., Upreti, B.N., Shrestha, S.D., 2001b. Core drilling of the basin-fill sediments in the Kathmandu Valley for palaeoclimatic study: preliminary results. Journal of Nepal Geological Society 25, 9-18.

Shakun, J.D., Burns, S.J., Fleitmann, D., Kramers, J., Matter, A., Al-Subary, A., 2007. A high-resolution, absolute-dated deglacial speleothem record of Indian Ocean climate from Socotra Island, Yemen. Earth and Planetary Science Letters 259, 442-456.

Schulz, H., von Rad, U., Erlenkeuser, H., 1998. Correlation between Arabian Sea and Greenland climate oscillations of the past 110,000 years. Nature 393,54-57.

Singer, A., 1984. The paleoclimatic Interpretation of Clay Minerals in sediments – a review. Earth-Science Reviews 21, 251-293.

Sinha, A., Cannariato, K.G., Stott, L.D., Li, H.-C., You, C.-F., Cheng, H., Edwards, R.L., Singh, I.B., 2005. Variability of southwest Indian summer monsoon precipitation during the Bølling-Allerød. Geology 33, 813-816.

Sirocko, F., Sarnthein, M., Lange, H., Erlenkeuser, H., 1991. Glacial to interglacial changes in Arabian Sea sediment accumulation rates: history of atmospheric summer circulation and coastal upwelling over the last 30,000 years. Quaternary Research 36, 72-93.

Sirocko, F., Sarnthein, M., Erlenkeuser, H., Lange, H., Arnald, M., Duplessy, J.C., 1993. Century-scale events in monsoonal climate over the past 24,000 years. Nature 364, 322-324.

Sirocko, F., Garbe-Schönberg, D., Devey, C., 2000. Geochemistry of Arabian Sea sediments during the last 25,000 years. Global and Planetary Change 26, 217-303.

Srodon, J., 1979. Correlation between coal and clay diagenesis in the Carboniferous of the Upper Silesian Coal Basin. Proceedings of the International Clay Conference. Oxford, pp. 251-260.

Srodon, J., Eberl, D.D., 1984. Illite. In: Bailey. S.W. (Ed.), Micas, Reviews in Mineralogy, Vol. 13. Mineralogical Society of America, pp. 495-544.

Tiwari, M., Ramesh, R., Somayajulu, B.L.K., Jull, A.J.T., Burr, G.S., 2006. Paleomonsoon precipitation deduced from a sediment core from the equatorial Indian Ocean. Geo-Marine Letters 26, 23-30.

Wang, P., Clemens, S., Beaufort, L., Braconnot, P., Ganssen, G., Jian, Z., Kershaw, P., Sarnthein, M., 2005. Evolution and variability of the Asian monsoon system: state of the art and outstanding issues. Quaternary Science Reviews 24, 595-629.

Yoshida, M., Igarashi, Y., 1984. Neogene to Quaternary lacustrine sediments in the Kathmandu Valley, Nepal. Journal of Nepal Geological Society 4, 73-100.

Figure Captions

Fig. 1. Outline geological map of the Kathmandu Basin showing the location of the Rabibhawan (RB) core (modified from Sakai, 2001).

Fig. 2. A columnar section of the RB core from 5 m – 45 m depth (modified from Sakai, 2001).

Fig. 3. An age-depth model of the RB core based on the AMS ^{14}C dating (above 30.1 m depth) and fine tuning of a pollen wet and dry index record to the SPECMAP $\delta^{18}O$ stack record with the LR04 age model (Lisiecki and Raymo, 2005) (below 30.1 m depth) (Hayashi et al., 2009; Mampuku et al., 2008; Hayashi, 2007).

Fig. 4. Decomposition with 5 elementary peaks of the XRD patterns obtained from AD sample of clay minerals in the RB core. The dotted lines represent observed profiles and solid lines calculated profiles. Gray lines represent the residuum.

Fig. 5. Variation records depicting (a) the amounts of clay fractions (< 2μm) in the RB core sediments, (b) illite crystallinity indices (Li and MLI), (c) the percentage of each clay mineral in the clay fraction, and (d) the amount of each clay mineral in sediments. The clay-poor zones (see text) are shaded.

Fig. 6. Representative XRD patterns of AD and EG samples of clay minerals in the

RB core.

Fig. 7. Correlation plots between (a) illite and kaolinite, (b) illite and I-S (R=1), (c) illite and smectite, (d) illite and MLI, (e) overall clay and illite, and (f) overall clay and kaolinite. Open marks indicate data points in the clay-poor zones and solid marks indicate those in the other. Symbol "*r*" in figure is a correlation coefficient, and "*F*" is a result of F test ($F = (n\text{-}2)\, r^2/(1\text{-}r^2)$, where "*n*" is the number of samples). In this test, random sampling (*n* = 90 selected from total number, *N* = 319, between 12 m and 45 m depth) was performed to each correlation plot to improve the power of F test and to avoid reducing of degrees of freedom in the records (Chelton, 1982). There is a correlation between the two elements when the *F* value is larger than the F^{1}_{88} (0.05) = 3.95.

Fig. 8. Comparison of the records of pollen dry index (Fujii, et al., 2004) and kaolinite/illite ratio (this study) for the Paleo-Kathmandu Lake sediments with the ISMI (30°N – 30°S, 1 July), NHSI (30°N, 1 July), SPECMAP $\delta^{18}O$ stack (Imbrie et al., 1984), $\delta^{18}O$ of the planktonic foraminifera *G. rubber* in sediment cores 88/93KL (Schulz et al., 1998) and Greenland GISP2 $\delta^{18}O$ ice record (Blunier and Brook, 2001). The records of pollen dry index and kaolinite/illite ratio are depicted based on the age model reconstructed using the sedimentation rates below 28 m depth of the RB core and a tie point between 47.5 m depth and 82.5 ka (see text) (solid lines), as well as based on the age-depth model of Hayashi et al. (2009), Mampuku et al. (2008) and Hayashi (2007) (dotted lines). Changes in sedimentary environment and paleoclimate in and around the Kathmandu Basin are also shown. Climates shown in parentheses in the paleoclimate box were indicated by Fujii et al. (2004). The dry climate zones are lightly shaded. Paleoclimate in the topmost part that is darkly shaded (8 ~ 17 ka) is uncertain (see text).

Fig. 9. (a) Cross-spectral analyses on the record of kaolinite/illite ratio with the NHSI at 1 July and the SPECMAP $\delta^{18}O$ stack. (b) Cross-correlation of the NHSI at 1 July, NHSI at 21 June, and SPECMAP $\delta^{18}O$ stack with the record of kaolinite/illite ratio. These analyses were done using the Analyseries software (Paillard et al., 1996).

Figure 1

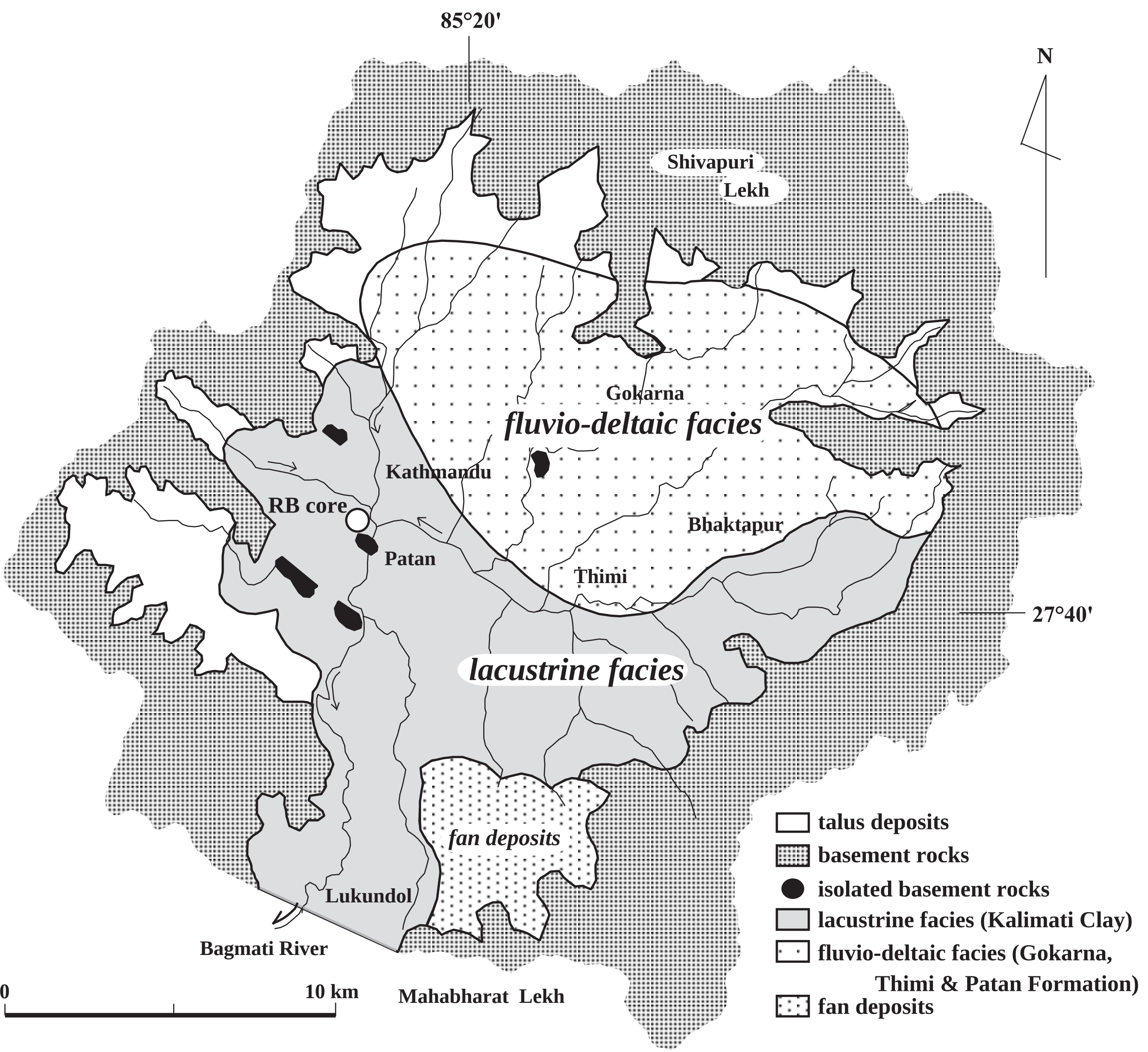
85°20'
N
Shivapuri
Lekh
Gokarna
fluvio-deltaic facies
Kathmandu
RB core
Patan
Bhaktapur
Thimi
27°40'
lacustrine facies
fan deposits
Lukundol
Bagmati River
0
10 km
Mahabharat Lekh
talus deposits
basement rocks
isolated basement rocks
lacustrine facies (Kalimati Clay)
fluvio-deltaic facies (Gokarna, Thimi & Patan Formation)
fan deposits

Figure 2

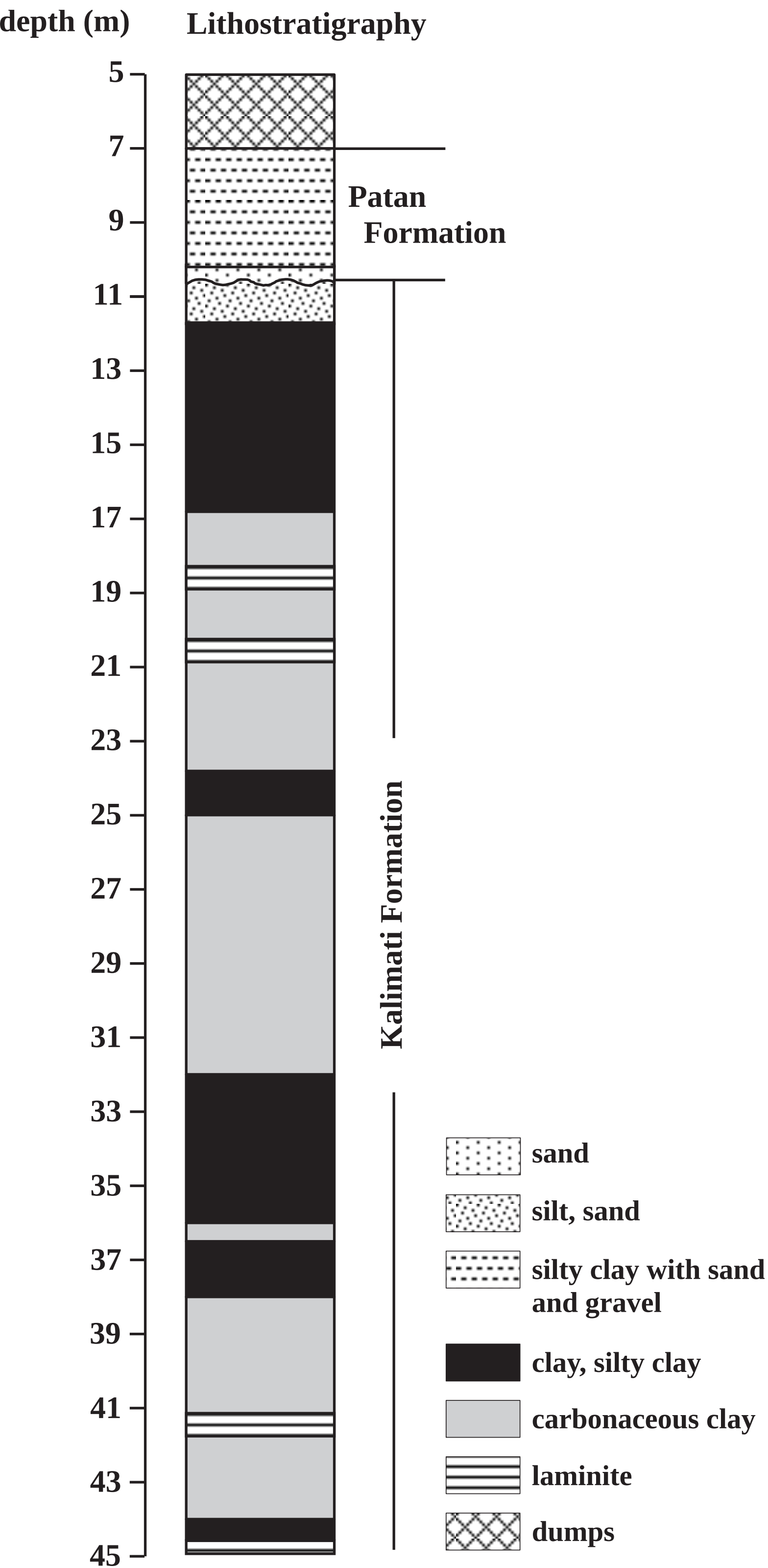
depth (m)
Lithostratigraphy
5
7
9
11
13
15
17
19
21
23
25
27
29
31
33
35
37
39
41
43
45
Patan Formation
Kalimati Formation
sand
silt, sand
silty clay with sand and gravel
clay, silty clay
carbonaceous clay
laminite
dumps

Figure 3

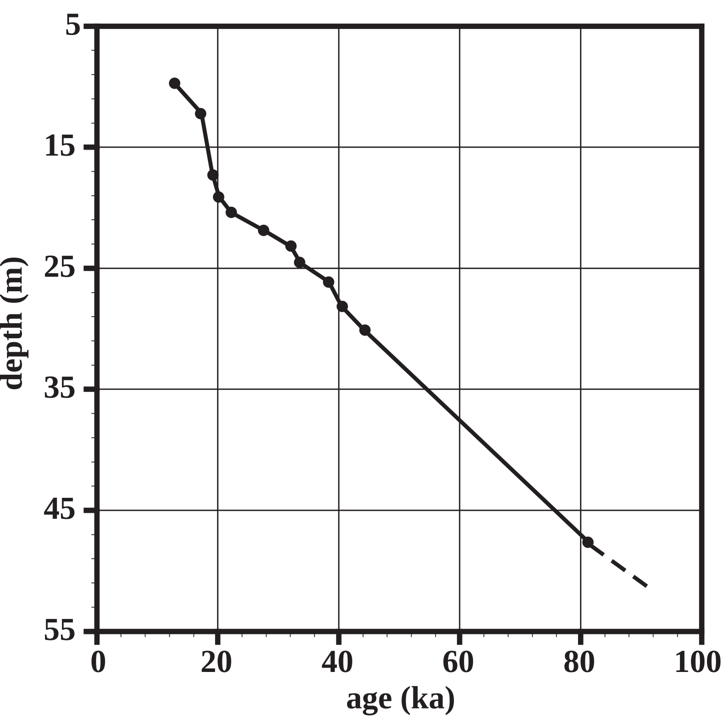

Figure 4

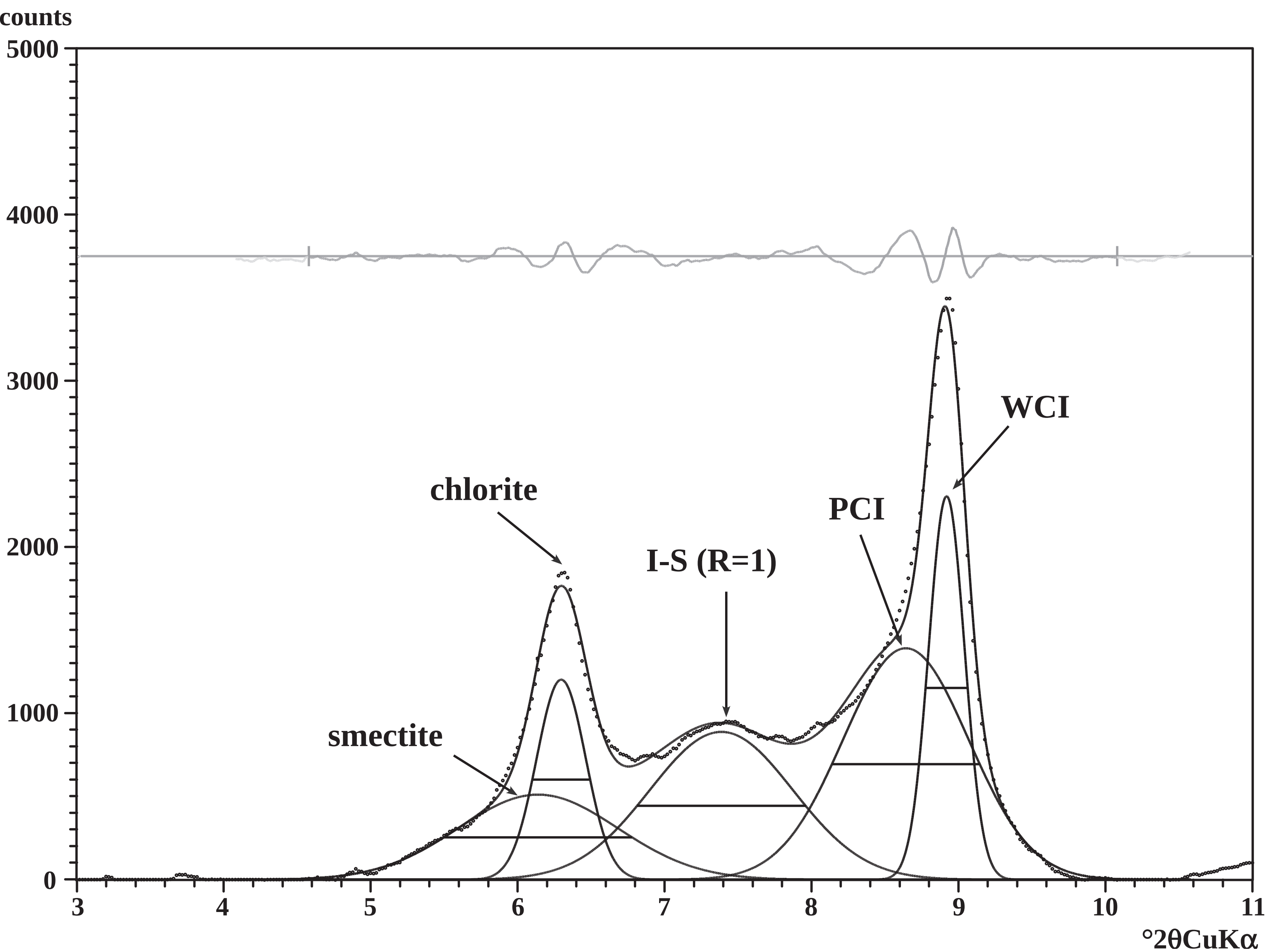
counts
5000
4000
3000
2000
1000
0
3
4
5
6
7
8
9
10
11
°2θCuKα
chlorite
smectite
I-S (R=1)
PCI
WCI

Figure 5

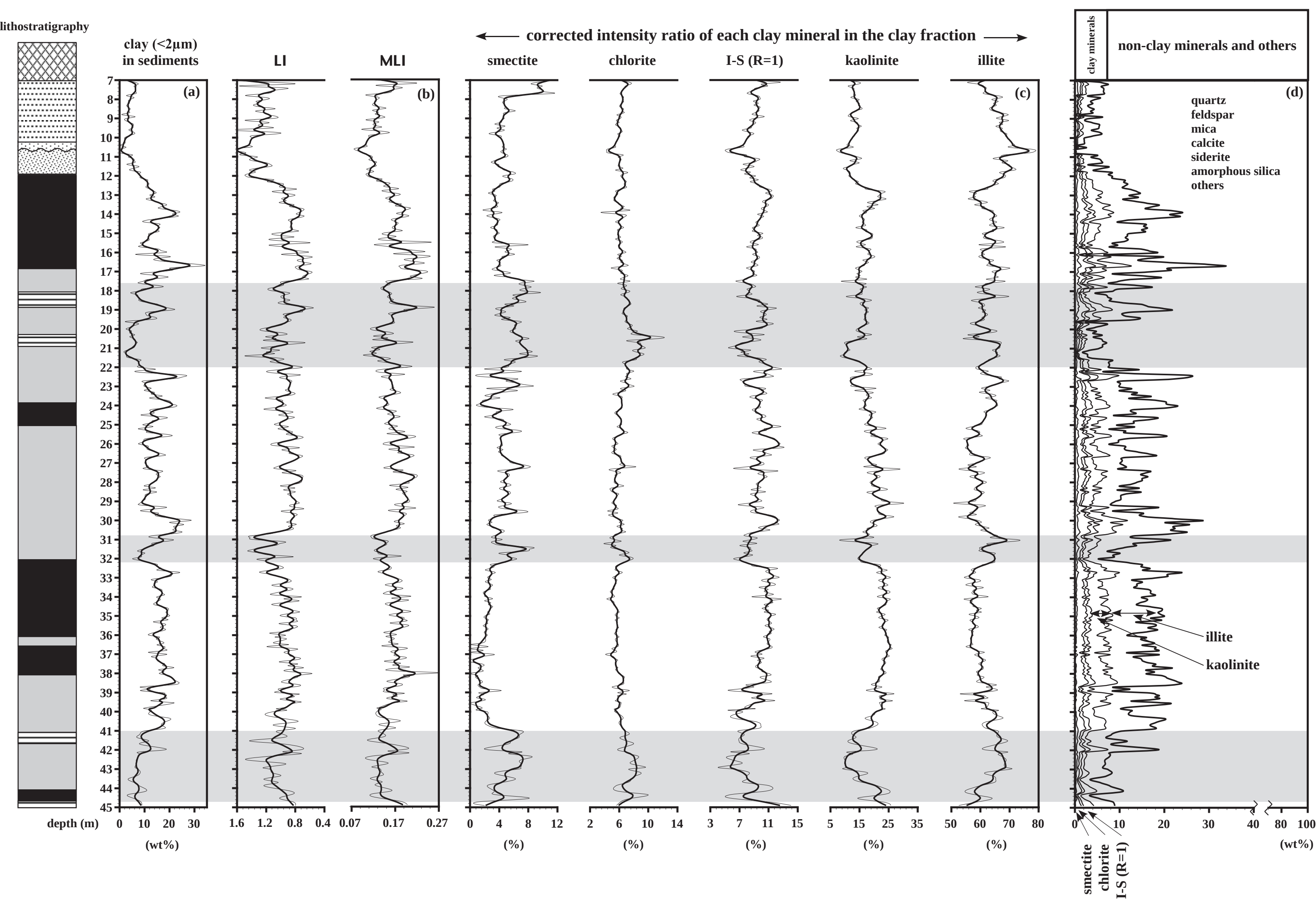

lithostratigraphy
clay (<2µm) in sediments
LI
MLI
corrected intensity ratio of each clay mineral in the clay fraction
smectite
chlorite
I-S (R=1)
kaolinite
illite
clay minerals
non-clay minerals and others
(a)
(b)
(c)
(d)
quartz
feldspar
mica
calcite
siderite
amorphous silica
others
illite
kaolinite
depth (m)
(wt%)
(%)
smectite
chlorite
I-S (R=1)

Figure 6

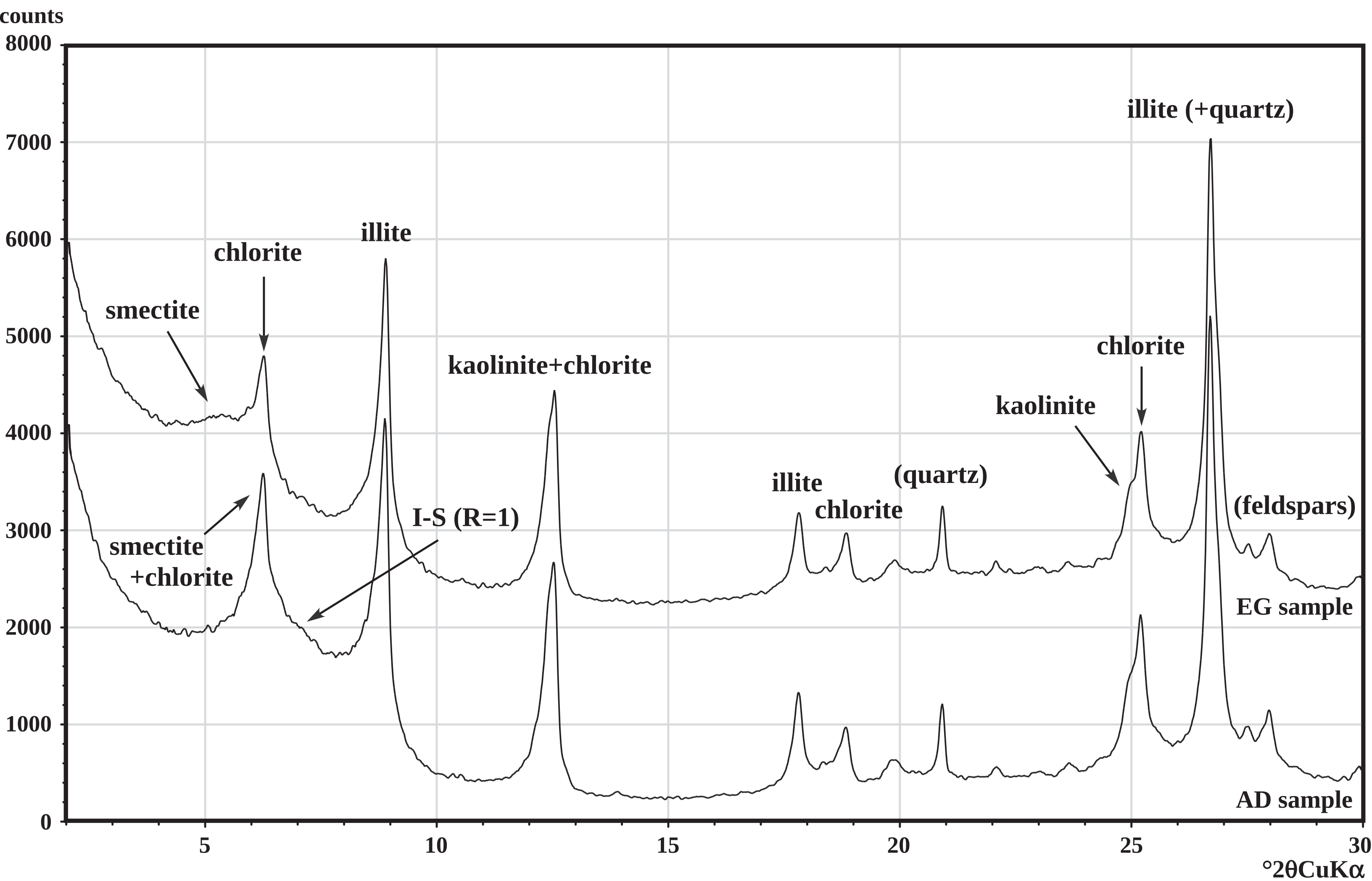
counts
8000
7000
6000
5000
4000
3000
2000
1000
0
5
10
15
20
25
30
°2θCuKα
smectite
chlorite
illite
kaolinite+chlorite
smectite
+chlorite
I-S (R=1)
illite
chlorite
(quartz)
kaolinite
chlorite
illite (+quartz)
(feldspars)
EG sample
AD sample

Figure 7
Click here to download high resolution image

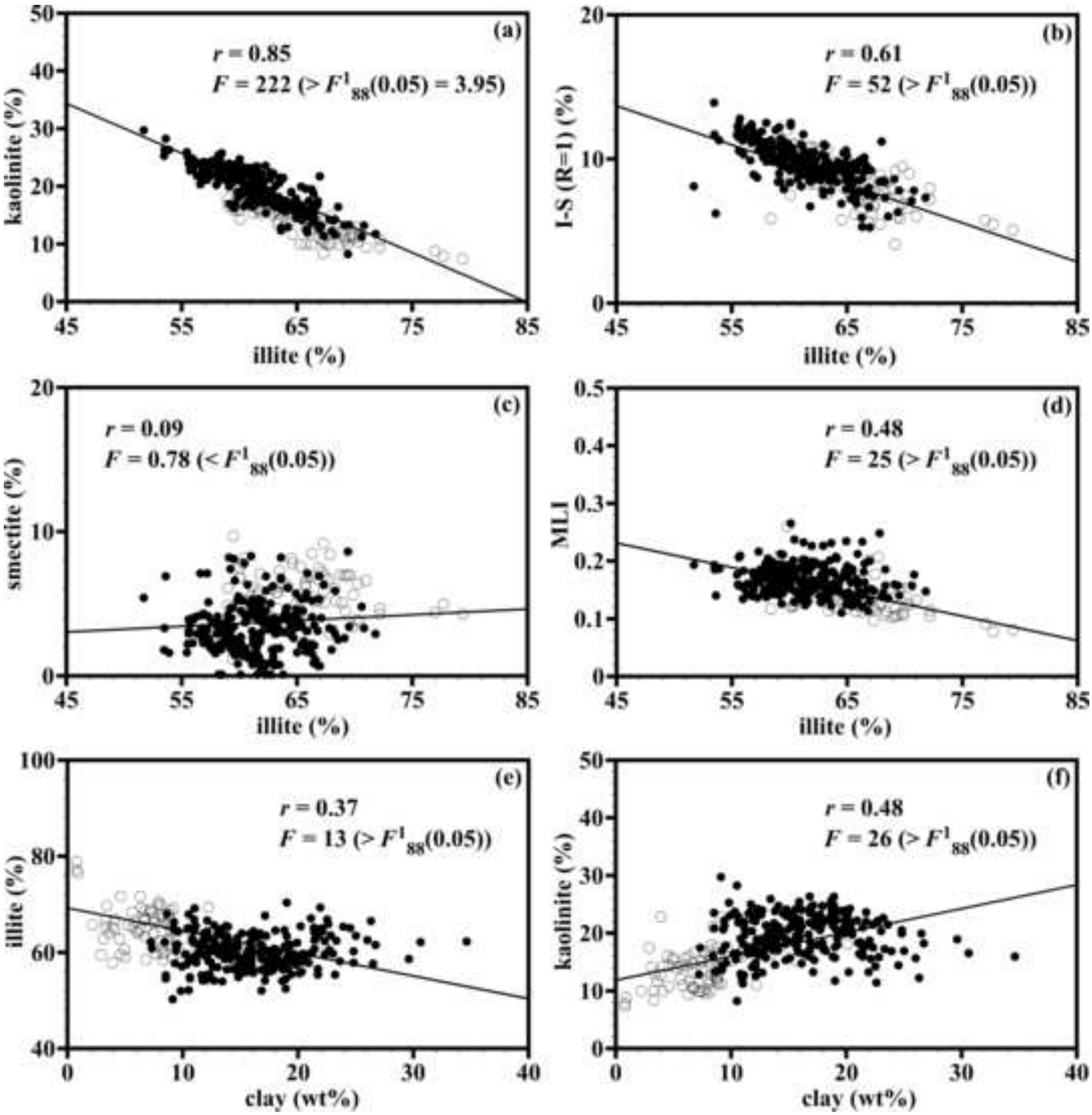

Figure 8

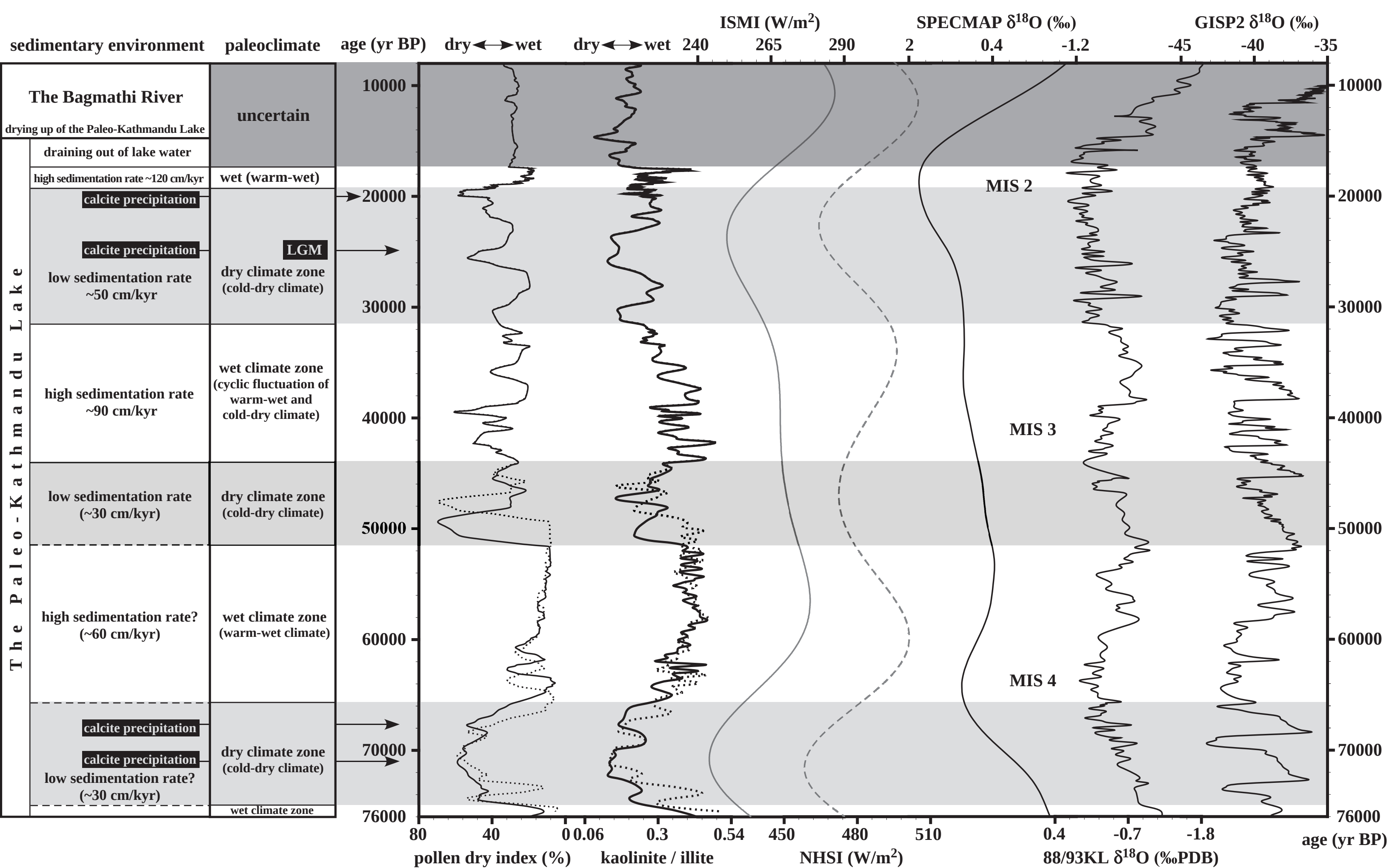

sedimentary environment
paleoclimate
age (yr BP)
dry ⟷ wet
dry ⟷ wet
ISMI (W/m2)
SPECMAP δ18O (‰)
GISP2 δ18O (‰)
240 265 290
2 0.4 -1.2
-45 -40 -35
The Bagmathi River
drying up of the Paleo-Kathmandu Lake
uncertain
draining out of lake water
high sedimentation rate ~120 cm/kyr
wet (warm-wet)
calcite precipitation
calcite precipitation
LGM
low sedimentation rate ~50 cm/kyr
dry climate zone (cold-dry climate)
high sedimentation rate ~90 cm/kyr
wet climate zone (cyclic fluctuation of warm-wet and cold-dry climate)
low sedimentation rate (~30 cm/kyr)
dry climate zone (cold-dry climate)
high sedimentation rate? (~60 cm/kyr)
wet climate zone (warm-wet climate)
calcite precipitation
calcite precipitation
low sedimentation rate? (~30 cm/kyr)
dry climate zone (cold-dry climate)
wet climate zone
The Paleo-Kathmandu Lake
MIS 2
MIS 3
MIS 4
10000 20000 30000 40000 50000 60000 70000 76000
80 40 0
0.06 0.3 0.54
450 480 510
0.4 -0.7 -1.8
age (yr BP)
pollen dry index (%)
kaolinite / illite
NHSI (W/m2)
88/93KL δ18O (‰PDB)

Figure 9

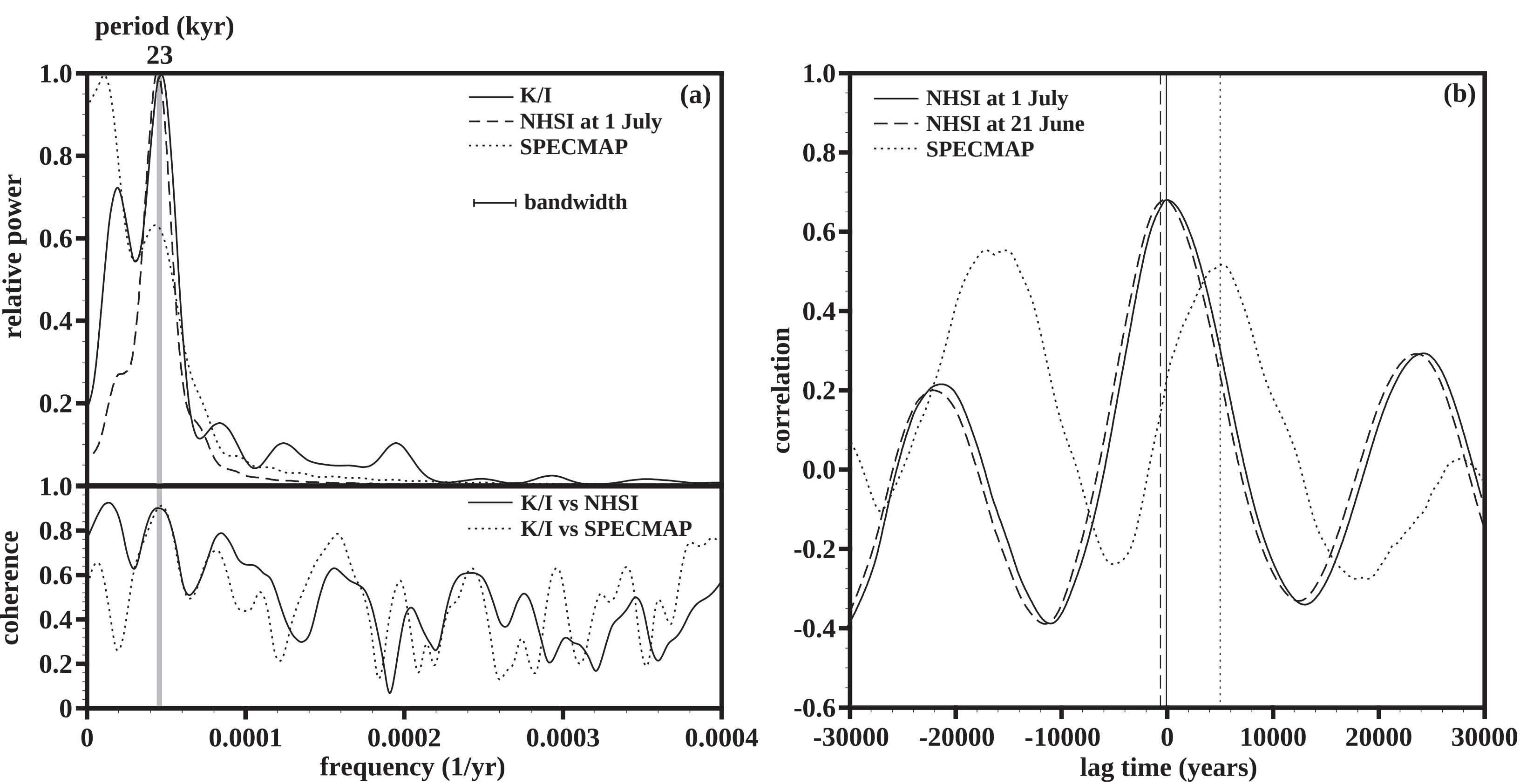

period (kyr)
23
(a)
K/I
NHSI at 1 July
SPECMAP
bandwidth
relative power
K/I vs NHSI
K/I vs SPECMAP
coherence
frequency (1/yr)
(b)
NHSI at 1 July
NHSI at 21 June
SPECMAP
correlation
lag time (years)